Journal of Testing and Evaluation

X. Cui,[1] X. Zhou,[2] J. Lou,[1] J. Zhang,[1] and M. Ran[3]

DOI: 10.1520/JTE20160040

Depth-from-Focus-Based 3D Reconstruction of Asphalt Pavement Micro-Texture

Journal of Testing and Evaluation

doi:10.1520/JTE20160040 available online at www.astm.org

TECHNICAL NOTE

X. Cui,[1] X. Zhou,[2] J. Lou,[1] J. Zhang,[1] and M. Ran[3]

Depth-from-Focus-Based 3D Reconstruction of Asphalt Pavement Micro-Texture

Reference

Cui, X., Zhou, X., Lou, J., Zhang, J., and Ran, M., "Depth-from-Focus-Based 3D Reconstruction of Asphalt Pavement Micro-Texture," *Journal of Testing and Evaluation* https://doi.org/10.1520/JTE20160040. ISSN 0090-3973

Manuscript received February 2, 2016; accepted for publication October 12, 2016; published online October 5, 2017.

[1] School of Civil Engineering, Shandong University, Jinan 250061, People's Republic of China

[2] School of Automobile and Traffic Engineering, Wuhan University of Science and Technology, Wuhan, Hubei 430081, China (Corresponding author), e-mail: zxl65@163.com

[3] School of Automobile and Traffic Engineering, Wuhan University of Science and Technology, Wuhan, Hubei 430081, People's Republic of China

ABSTRACT

Three-dimensional image reconstruction is one of the basic methods to obtain the micro-texture characteristics of body surface. In this study, a novel 3D-reconstruction measurement technique is proposed to rapidly and reliably capture the features of asphalt pavement micro-texture. This technique is based on the depth-from-focus principle. Sequential images of pavement texture are hierarchically photographed using a monocular stereo microscope installed perpendicularly to the surface of asphalt specimen. These images focus on different depths of the pavement surface, and each pixel on the clear area of the images are orientated and combined into a fused image through the new proposed algorithm, which introduces the improved Laplacian focus operator. The three-dimensional picture of micro-texture can be reconstructed utilizing the MATLAB software with the altitude data of the pixels obtained through the Gaussian interpolation. Laboratory tests are described and the results exhibit that the proposed method can accurately reconstruct the three-dimensional micro-texture of asphalt pavement.

Keywords

asphalt pavement, micro-texture, 3D reconstruction, depth-from-focus, machine vision

Introduction

The micro-texture of asphalt pavement surface is an essential factor that influences the pavement performances, including skid resistance and noise reduction [1,2]. Micro-texture acquisition is the basic of the researches on micro-texture feature parameters, which lays the foundation for pavement material design and pavement performance researches. Besides the traditional contact-measuring methods of micro-texture depth, such as the sand patch method and the outflow meter, current science tends to pursue precise imaging techniques with highly automated apparatus to evaluate the asphalt pavement micro-texture, which is mainly referred to the category of machine vision.

In recent years, predecessors have made several attempts on the studies of non-contact measuring techniques for micro-texture. Five typical measuring methods in the realm of machine vision have formed and developed, including the binocular stereoscopy, the laser scanning, the shape acquisition from shadow, the depth-from-defocus, and the depth-from-focus technology [3]. The photometric stereo technology belongs to the category of the binocular stereoscopy [4–6]. In this technology, a micro-texture data-acquisition system is established with a light source and several photographic apparatus to recover the pavement surface texture three-dimensionally [7–9]. The circular track meter (CTM) is a type of laser-based device that introduces the laser scanning technique to reduce the instability of measurement system created by the light source [10,11]. Bubaker-Isheil et al. has also described a measuring system that consists of an additional 3D laser scanner and a coordinate measurement machine (CMM) [12]. This system breaks through the limitation of the presence of markers on the observed objects and enhances the accuracy of the image pixels. However, in the long-term practice of asphalt pavement engineering, the emerging techniques mentioned above have not been extensively used for cost efficiency and the equipment feasibility reasons.

Among the five measuring methods, nevertheless, the depth-from-focus technique has drawn little attention and almost remains a blank area for the measurement of asphalt pavement micro-texture [13]. In this study, a microscopic three-dimensional measurement method based on the depth-from-focus principle is developed for asphalt pavement micro-texture data acquisition. Combined with the procedure of 3D-reconstruction, the stereo image of asphalt pavement surface can be recovered. Because of its high speed and efficiency, this novel technique exhibits an enormous potential in the engineering practice of asphalt pavement construction and monitoring.

Experiment Program

THE MEASUREMENT SYSTEM

The measurement apparatus is shown in **Fig. 1**. A monocular stereo microscope is the central unit of the micro-texture measurement system. This microscope is equipped with a photographic device (CCD camera), which is designed to film the sequential images of the observed object and automatically recorded the Z-coordinate of each frame. The stereo microscope magnification is set on 50×. The focal plane is regulated on the reference plane, which is 5 mm below the top of the specimen. A stepping motor is controlled to move up along the precise guide rail and take a 576×768 picture every 50 µm. After that, the microscope is put back to the original position. The field of view is 2.98 mm × 3.92 mm. 100 frames of images are acquired and the calculation window of focal operator is set as 9×9. The pictures of the asphalt surface texture are captured by a CCD camera and transmitted to the computer for image processing. As shown in **Fig. 1**, the sequential images i ($I = 1, 2, 3, 4, \ldots, n$) are obtained with the step length δ. The texture depth information is contained in all the images. Assuming that a certain region on the ith image of the image sequence is clear, this is the region that locates on the focal plane, whose height of Z-direction is $\delta \times i$. The pixels in the clear area can be recognized by the focal algorithm described later, and fused into a single image. Thereby, the full-focus image that is totally clear through the entire depth of field can be reconstructed. Through the mathematical process of focal analysis as well as interpolation and fitting, the depth value of every point on the image can be accurately recovered. Finally, through the principle of machine vision imaging, the space coordinates of each point can be computed and the procedure of micro-texture three-dimensional reconstruction is completed.

FIG. 1 Measurement apparatus.

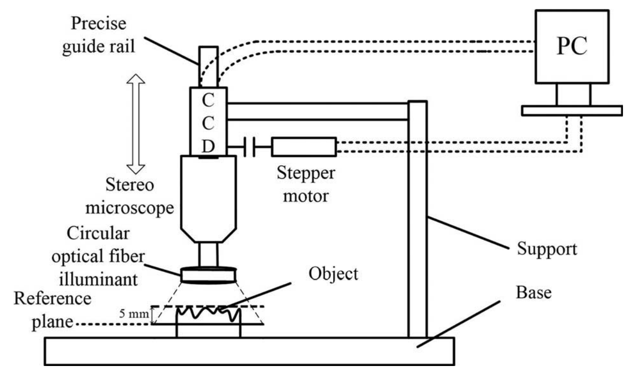

To be specific, as mentioned before, the focus position of each pixel on the image is identified by controlling the microscope. It is noted that the optical microscope is a device with a very small depth of field. That produces clear areas of the image containing the clear pixels that should be recorded. The altitudes of these clear pixels can be determined according to the focal plane's height. The Z-axis spacing of the microscope should be set smaller than the depth of field to locate all of the pixels on the corresponding layers. As a result, a full-focus image can be obtained. **Fig. 2** shows the brief principle of capturing sequential images.

FIG. 2 Brief principle of capturing sequential images.

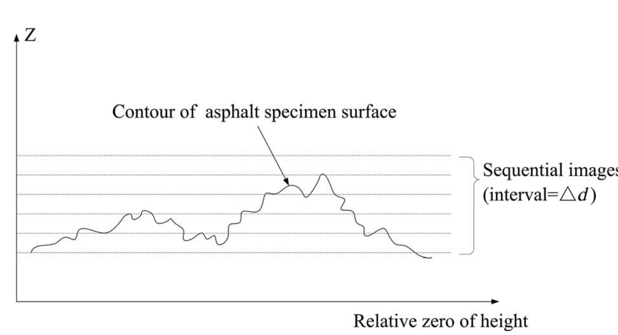

THREE-DIMENSIONAL RECONSTRUCTION

To realize the three-dimensional reconstruction, it is necessary to establish a mathematical relationship between the image points and the object points. Based on the pinhole imaging principle, the principal point, the object point, and the image point are collinear and satisfy the collinearity equation (Eq 1).

$$\begin{cases} x - x_0 = -f\dfrac{a_1(X - X_S) + b_1(Y - Y_S) + c_1(Z - Z_S)}{a_3(X - X_S) + b_3(Y - Y_S) + c_3(Z - Z_S)} \\ y - y_0 = -f\dfrac{a_2(X - X_S) + b_2(Y - Y_S) + c_2(Z - Z_S)}{a_3(X - X_S) + b_3(Y - Y_S) + c_3(Z - Z_S)} \end{cases} \tag{1}$$

where:

x_0, y_0 = the coordinates of the principal point projection in the photo plane,

f = the vertical distance from the principal point to the photo plane,

these three parameters = the interior orientation elements,

x, y = the coordinates of the image points projection in the image space,

X_s, Y_s, Z_s = the geodetic coordinates of the principal point,

X, Y, Z = the geodetic coordinates of the image points, and

a_i, b_i, c_i (I = 1, 2, 3) = the external orientation elements, which are the coefficients of the rotation matrix constituted by three angle parameters.

Equation 1 can be transformed into the form of direct linear transformation (DLT), as shown in Eq 2. This method is the solution to calculate the image plane coordinates of the image points and the geodetic coordinates of the corresponding object points.

$$\begin{cases} \bar{x} + \dfrac{l_1X + l_2Y + l_3Z + l_4}{l_9X + l_{10}Y + l_{11}Z + 1} = 0 \\ \bar{y} + \dfrac{l_5X + l_6Y + l_7Z + l_8}{l_9X + l_{10}Y + l_{11}Z + 1} = 0 \end{cases} \tag{2}$$

where:

$\bar{x}$ and $\bar{y}$ = the image plane coordinates of the image points. Equation 2 can be transformed into Eq 3.

$$\begin{cases} (l_1 + \bar{x}l_9)X + (l_2 + \bar{x}l_{10})Y + (l_3 + \bar{x}l_{11})Z + (l_4 + \bar{x}) = 0 \\ (l_5 + \bar{y}l_9)X + (l_6 + \bar{y}l_{10})Y + (l_7 + \bar{y}l_{11})Z + (l_8 + \bar{y}) = 0 \end{cases} \tag{3}$$

where:

l_1, l_2, l_3,…, l_{10}, l_{11} = the undetermined parameters of the monocular stereo microscope, which are identified by calibration.

Considering the influence from the distortion error of the lens, Eq 4 is acquired.

$$\begin{cases} \bar{x} = x + \Delta x = x + (x - x_0)r^2k_1 \\ \bar{y} = y + \Delta y = y + (y - y_0)r^2k_1 \end{cases} \tag{4}$$

Plug Eq 4 in to Eq 3, and the values of X, Y can be computed as Eq 5.

$$\begin{cases} X = \dfrac{[(l_2l_7 - l_6l_3) + (l_7l_{10} - l_6l_{11})[x + (x - x_0)r^2k_1] + (l_2l_{11} - l_3l_{10})[y + (y - y_0)r^2k_1]]Z + (l_2l_8 - l_4l_6) + (l_8l_{10} - l_6)[x + (x - x_0)r^2k_1] + (l_2 - l_4l_{10})[y + (y - y_0)r^2k_1]}{(l_1l_6 - l_2l_5) + (l_6l_9 - l_5l_{10})[x + (x - x_0)r^2k_1] + (l_1l_{10} - l_2l_9)[y + (y - y_0)r^2k_1]} \\ Y = \dfrac{[(l_3l_5 - l_1l_7) + (l_5l_{11} - l_7l_9)[x + (x - x_0)r^2k_1] + (l_3l_9 - l_1l_{11})[y + (y - y_0)r^2k_1]]Z + (l_4l_5 - l_1l_8) + (l_5 - l_8l_9)[x + (x - x_0)r^2k_1] + (l_4l_9 - l_1)[y + (y - y_0)r^2k_1]}{(l_1l_6 - l_2l_5) + (l_6l_9 - l_5l_{10})[x + (x - x_0)r^2k_1] + (l_1l_{10} - l_2l_9)[y + (y - y_0)r^2k_1]} \end{cases} \tag{5}$$

where:

k_1, k_2 = symmetrical radial distortion coefficients, and

$$r = [(x - x_0)^2 + (y - y_0)^2]^{1/2}.$$

Based on the technology of depth-from-focus, the depth information $\bar{d}$ of each image point (x, y) can be obtained through the sequential images processing. The Z-coordinates are

$$Z = \bar{d} \tag{6}$$

According to Eqs 5 and 6, Eq 7 with the only independent variable $\bar{d}$ can be determined:

$$\begin{cases} X = \mathrm{f}(\bar{d}) \\ Y = \mathrm{g}(\bar{d}) \\ Z = \bar{d} \end{cases} \tag{7}$$

Up to this point, we have established a math relationship between the image point (x, y) and its geodetic coordinate (X, Y, Z), the mathematical procedure of three-dimensional reconstruction is completed.

Calculation Method of Texture Depth

The micro-texture depth information is obtained through the depth-from-focus technology. In this respect, there are two problems remain to be solved: (1) to select an effective discrimination factor to recognize the clear area of the image, called the focal algorithm; and (2) calculation of the depth information.

FOCAL ALGORITHM

Multi-layer sequential image fusion is implemented to generate a panoramic picture [14,15], of which the basic idea is to use a suitable focus algorithm to recognize the clear area of the images and integrate them into the picture layers, as shown in **Fig. 3**.

Presently, there are two types of fusion algorithms: point processing and regional processing [16,17]. The direct fusion operator method, the grayscale average method, and the maximum deviation method belong to the point processing, which are not accurate enough and are restricted in application.

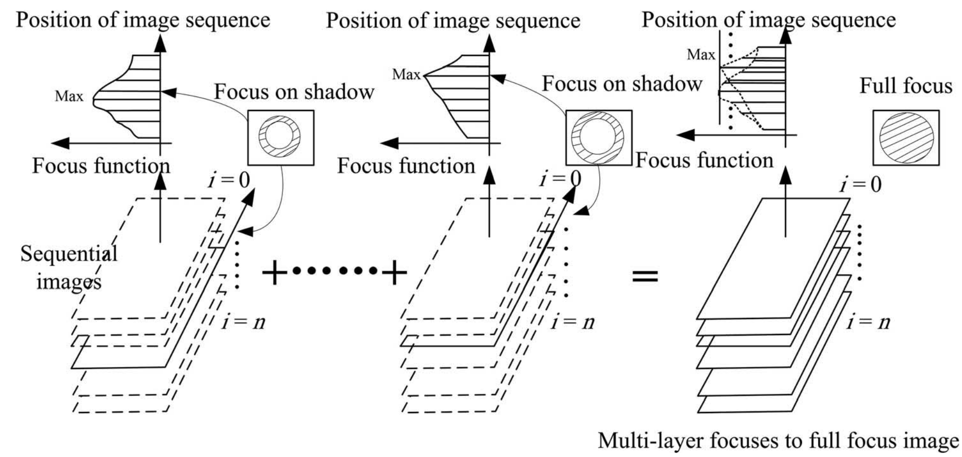

FIG. 3
Basic principles of microscopic image sequence fusion.

The algorithm based on the regional processing is to set an $M \times N$ window centering a certain pixel, and making calculation in this window. The sum of mean, maximum, and minimum gray values of the image inside the window is used to judge whether the pixels are selected as the final pixel in the fused image. The operators of Laplacian, Tenegrad, variance, and average focus measuring are the common algorithms in the category of the regional processing. These measuring operators can quantitatively evaluate the degree of image focus [1].

Asphalt surface has abundant textural features and high roughness, of which sharp edges exist in the clear images. The Laplacian operator is a linear combination of second derivatives, which is a common second-order detect operator in two-dimensional pictures. The second derivatives can deduce high-frequency components, so that the sharp-edge contours can be obtained. The modified Laplacian operator is more reliable to more quickly recognize the clear area of the image, and make up an improved image fusion algorithm under the variability of texture.

Take the sum of the absolute values of second derivatives, as shown in Eq 8.

$$\nabla^2 f(x,y) = \left|\frac{\partial^2 f(x,y)}{\partial x^2}\right| + \left|\frac{\partial^2 f(x,y)}{\partial y^2}\right| \tag{8}$$

Generally, the modified Laplacian operator is approximated a 3×3 operator when being used in the image processing. The size of the window is controlled according to the changes of the actual micro-picture. Assuming that the size of the window is $M \times N$ and variable step L of the pixels is applied with difference computing instead of differential, the ultimate form of the evaluation function $F(i, j)$, which is used to evaluate whether the pixel is effective in clear area, can be expressed as Eqs 9 and 10.

$$F(i,j) = \sum_{x=i-N}^{i-N} \sum_{y=j-M}^{j+M} ML(x,y) \quad \text{when} \quad ML(x,y) > T \tag{9}$$

$$ML(x,y) = |2f(x,y) - f(x-L,y) - f(x+L,y)| + |2f(x,y) - f(x,y-L) - f(x,y+L)| \tag{10}$$

where:

T = the threshold of the Laplacian value.

Only if bigger than T can the Laplacian value be involved in the calculation. The threshold aims to remove the noise signal.

The Laplacian operator is the second-order difference, which increases the impact of high-frequency noise on accuracy. Experiments show that the application of the threshold and the variable step in the modified Laplacian operator can restrain the high-frequency noise effectively.

The step length and threshold are determined according to the actual conditions. The fused images with the modified Laplacian operators are shown in Fig. 4a–4c.

The first parameter in the bracket presents the size of window; the second presents the step length L of the Laplacian operator, which is usually selected as 5; the third parameter presents the threshold T, smaller than which the value of Laplacian operator should be ignored. In Fig. 4, the fusion image with the parameter (2,5,0) is the clearest; the fusion image with the parameter (5,5,0) is similar to the former, while the fusion image with the parameter (5,2,0) is quite different, whose edge is rough and blurred. As a result, the impact of step length is larger than the size of window on fusion images. In conclusion, the step length should be set longer and the size of the window should be smaller in image processing.

CALCULATION OF TEXTURE DEPTH

To recover the three-dimensional information from the two-dimensional picture, it is needed to get the texture depth data first, and then determine the shape of the specimen. Fitting and interpolation is the way to implement the three-dimensional reconstruction. The Gaussian interpolation is applied because the modified Laplacian operator focal values present normal distribution near the peak value [18].

FIG. 4 The influence of step length and window size on the fusion effect.

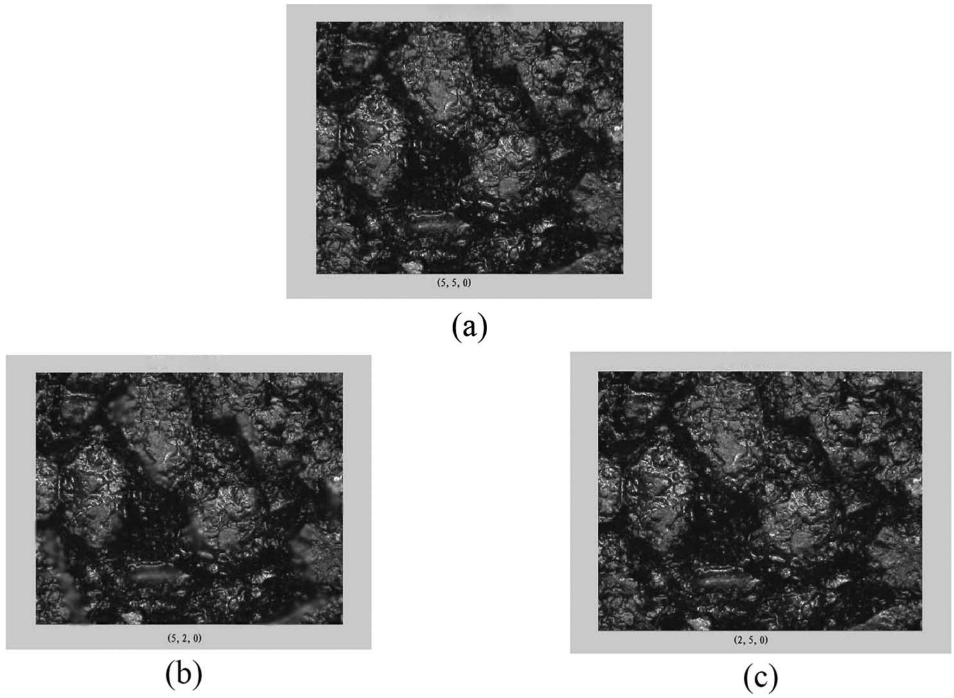

How to precisely recover the value of texture depth $\overline{d}$ through focus evaluation functions and the Gaussian interpolation is the topic discussed below. Three values of the focus evaluation function near the maximum are selected for the Gaussian interpolation, as shown in **Fig. 5**.

In **Fig. 5**, $\overline{d}$ presents the actual height of the point, which is corresponding to the focal operator value F_p. F_m is the maximum value of focal operator calculated by the picture information. d_m is the focal plane height that is corresponding to the layer of F_m, F_{m+1} and F_{m-1} are the focal operators near F_m, which satisfy $F_m \geq F_{m+1}$, $F_m \geq F_{m-1}$. According to the Gaussian distribution, the focus function can be presented as Eq 11.

FIG. 5 Gaussian interpolation.

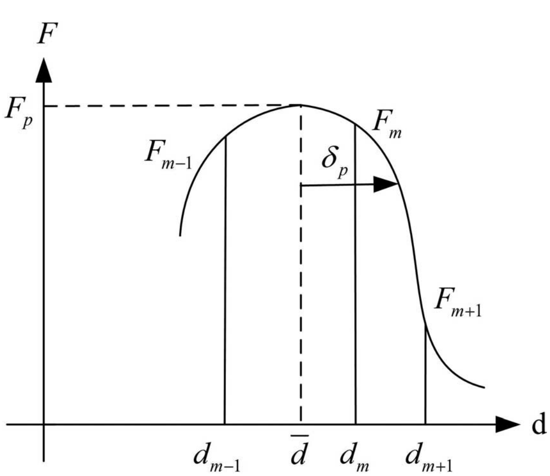

$$F = F_P \exp\left[-\frac{1}{2}\left(\frac{d-\overline{d}}{\sigma_p}\right)^2\right] \tag{11}$$

where:

σ_p = the standard deviation of the Gaussian distribution.

In logarithm:

$$\ln F = \ln F_P - \frac{1}{2}\left(\frac{d-\overline{d}}{\sigma_p}\right)^2 \tag{12}$$

To plug F_m, F_{m+1}, F_{m-1} and d_m, d_{m+1}, d_{m-1}, and the step Δd into Eq 12, Eq 13 can be obtained:

$$\overline{d} = \frac{(\ln F_m - \ln F_{m+1})(d_m^2 - d_{m-1}^2)}{2\Delta d[(\ln F_m - \ln F_{m-1}) + (\ln F_m - \ln F_{m+1})]} - \frac{(\ln F_m - \ln F_{m-1})(d_m^2 - d_{m+1}^2)}{2\Delta d[(\ln F_m - \ln F_{m-1}) + (\ln F_m - \ln F_{m+1})]} \tag{13}$$

Comparison Test

To validate the micro-textures obtained by the novel technique, the contour line of the asphalt sample was measured using a laser profiler for comparison. The asphalt sample in this test was AC-16C material taken from the G35 Expressway in Hubei Province in China, of which the asphalt-aggregate ratio is 4.5 % and the mineral powder content is 3.5 %. The aggregate grading is shown in **Fig. 6**.

FIG. 6 Aggregate grading.

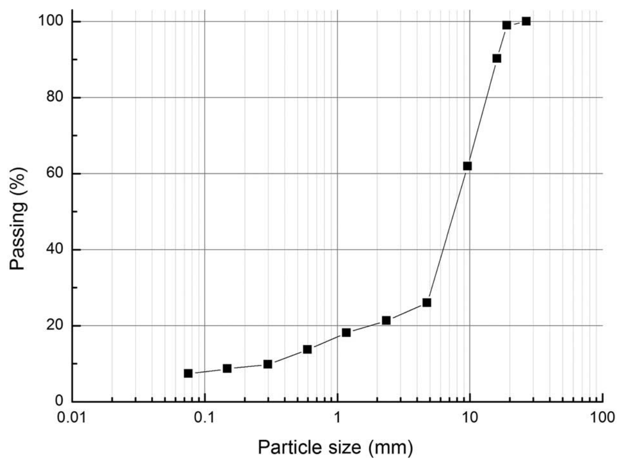

The measure system was calibrated by the direct linear transformation (DLT) method. Fig. 7a–7c presents a part of the sequential images of asphalt sample. Fig. 7a focuses on the lower layer and Fig. 7c focuses on the top layer. Fig. 7d is the full-focus image after fusing 100 frames of sequential images.

The MATLAB software is used to finish the numerical work of image fusion and 3D-reconstruction of micro-texture through the algorithms proposed. Reconstruction effect is shown in Fig. 8.

The measuring accuracy of laser profile is 1 μm and its resolution is 0.1 μm, which satisfies the request of the comparison with the new method. One profile extracted from the reconstruction image is shown in Fig. 9a. The same profile obtained from the laser profiler is shown in Fig. 9b. Table 1 lists the coordinates of a part of 100 points on the profile of the two method and their error values. In consideration of space, we just list the coordinates corresponding to the abscissa scales in Fig. 9. The evaluation error can be evaluated by the average values of root-mean-squares, as shown in Eq 14.

$$E_k = \frac{1}{N}\sum_{i=1}^{N}\sqrt{(X_i - X_{Wi})^2 + (Y_i - Y_{Wi})^2 + (Z_i - Z_{Wi})^2} \quad (14)$$

where:

X_i, Y_i, Z_i = the coordinates measured by the new method,
X_{Wi}, Y_{Wi}, Z_{Wi} = the coordinates measured by laser profiler, and
E_k = the evaluation error that reflects the precision of the new method.

FIG. 7 Sequential images of asphalt sample.

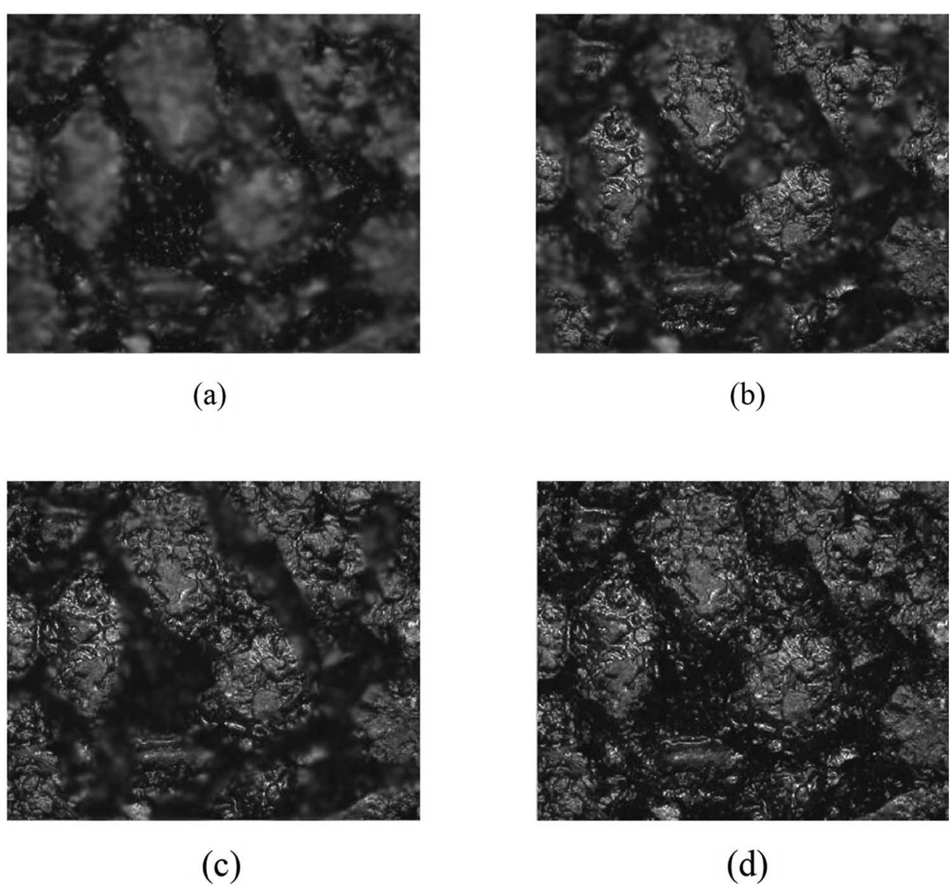

FIG. 8
Reconstruction effect.

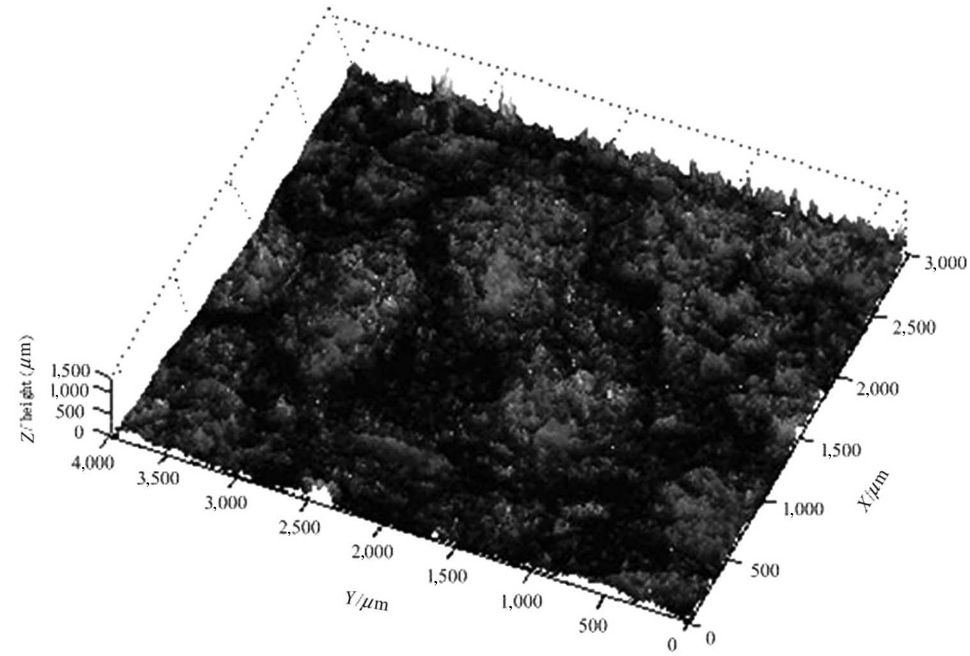

FIG. 9
Profile sample.

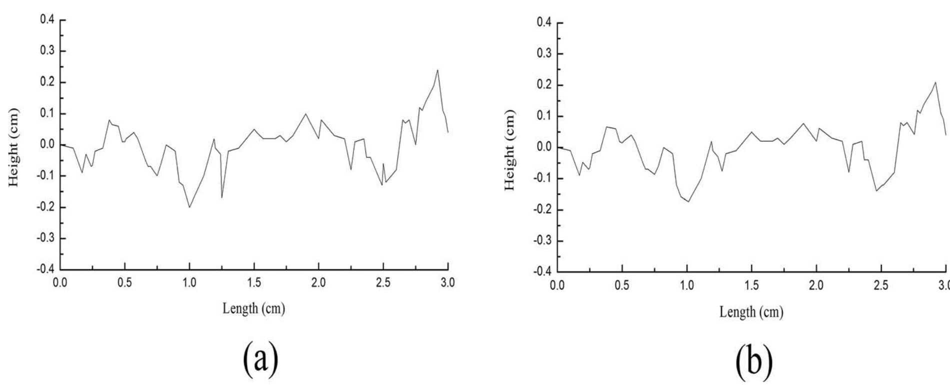

This can be drawn from the 100 coordinates listed in **Table 1**: $E_k = 0.0187$. This small margin of error means that the result of the new method is close to the physical truth. The shapes of the profiles from the two methods are generally the same, and the new method is more elaborate at some local positions.

Repetitive tests were conducted 100 times and the average time cost of the whole process, including photographing and numerical computing, is 2 s, almost 0.02 s for each frame. That means the proposed method satisfies the request of rapid measurement and can be further developed into on-board measurement system.

The experiment above shows that the three-dimensional reconstruction technology of sequential images can well reconstruct the stereo appearance of micro-texture. There are several notes for further application of the developed method:

1. The method is implemented by collecting sequential images to reconstruct the micro-texture, which is more reliable than by a single image. The measurement has strict requirement of illumination, and only in evenly illuminative areas can the best view effect of micro-texture be acquired at the focus. For this concern, the circular optical fiber illuminant should be applied in the measurement.
2. The method of the depth-from-focus is suitable for convex texture with the vertical angles smaller than 90°. Against the rich-textured asphalt specimen that has vertical angles

TABLE 1 Coordinates of the two methods (mm).

Laser Profiler	Depth from Focus	Error
(0.0000, 1.0000, 0.0000)	(0.0000, 1.0000, 0.0000)	(0.0000, 0.0000, 0.0000)
(0.2500, 1.0000, −0.0456)	(0.2500, 1.0000, −0.0735)	(0.0000, 0.0000, 0.0279)
(0.5000, 1.0000, 0.0138)	(0.5000, 1.0000, 0.0125)	(0.0000, 0.0000, 0.0013)
(0.7500, 1.0000, −0.0825)	(0.7500, 1.0000, −0.1025)	(0.0000, 0.0000, 0.0200)
(1.0000, 1.0000, −0.1525)	(1.0000, 1.0000, −0.2025)	(0.0000, 0.0000, 0.0500)
(1.2500, 1.0000, −0.1132)	(1.2500, 1.0000, −0.1465)	(0.0000, 0.0000, 0.0333)
(1.5000, 1.0000, 0.0009)	(1.5000, 1.0000, 0.0015)	(0.0000, 0.0000, 0.0006)
(1.7500, 1.0000, 0.0278)	(1.7500, 1.0000, 0.0495)	(0.0000, 0.0000, 0.0217)
(2.0000, 1.0000, 0.0756)	(2.0000, 1.0000, 0.0845)	(0.0000, 0.0000, 0.0089)
(2.2500, 1.0000, 0.0425)	(2.2500, 1.0000, 0.0023)	(0.0000, 0.0000, 0.0402)
(2.5000, 1.0000, −0.0532)	(2.5000, 1.0000, −0.0972)	(0.0000, 0.0000, 0.0440)
(2.7500, 1.0000, 0.1142)	(2.7500, 1.0000, 0.1458)	(0.0000, 0.0000, 0.0316)
(3.0000, 1.0000 0.1842)	(3.0000, 1.0000, 0.2575)	(0.0000, 0.0000, 0.0733)

bigger than 90°, mathematical processing of interpolation should be applied for approximation.

3. In the software process, the modified Laplacian operator can be fused with the wavelets for accuracy enhancement of three-dimensional reconstruction. The step length of the sequential images acquisition should be a bit smaller than the field of view. The smaller the step length is, the more the images can be acquired, which means the higher precision of the fusion image can be obtained with higher requirements of data processing. On the hardware side, the guide rail of the microscope should be machined more precisely. Laser distance meter can be employed for the stepping motor to get a perfectly accurate step length.

Conclusions

A high-precision method of asphalt pavement micro-texture three-dimensional reconstruction is developed based on the depth-from-focus principle. This method solves the problem of three-dimensional micro-texture recognition and extraction. The experiment implemented on asphalt specimens is simple and reliable; the precision of micro-texture feature parameters has reached 50 μm. The present technique can satisfy the precision of 0.1 μm. 0.01 μm is also available if the test devices can be improved. This method fully meets the requirement of the researches on pavement noise-reduction, skid-resistance, and engineering practice.

ACKNOWLEDGMENTS

This work is supported by the National Program on Key Basic Research Project of China (973 Program) (No. 2015CB058101), the Science Fund for Distinguished Young Scholars of Shandong Province (No. JQ201416), the Natural Science Foundations of China (Nos. 51578430, 51479105, 51279094, 51308324, and 51379115), the Program for New Century Excellent Talents in University of Ministry of Education of China (NCET-13-0340), the Fundamental Research Funds of Shandong University (No. 2014YQ013), the China Postdoctoral Science Foundation (No. 2014M561761), the Natural Science Foundations of Hubei (2015CFA064), and the Science and Technology Support Plan of Hubei Province (2014BEC055).

References

[1] Fletcher, T., Chandan, C., Masad, E., and Sivakumar, K., "Measurement of Aggregate Texture and Its Influence on Hot Mix Asphalt (HMA) Permanent Deformation," *J. Test. Eval.*, Vol. 30, No. 6, 2002, pp. 524–531.

[2] Wang, W., Yan, X., Huang, H., Chu, X., and Abdel-Aty, M., "Design and Verification of a Laser Based Device for Pavement Macrotexture Measurement," *Transport. Res. Part C, Emerg. Technol.*, Vol. 19, No. 4, 2011, pp. 682–694, https://doi.org/10.1016/j.trc.2010.12.001

[3] Liu, L., Jiang, Z., Xie, F., and Chen, J., "Research and Development of Stereoscopic System Based on Stereo Light Microscope Image," *Chinese J. Stereol. Image Anal.*, Vol. 8, No. 4, 2003, pp. 220–224.

[4] Ergun, M., Lyinam, S., and Lyinam, A. F., "Prediction of Road Surface Friction Coefficient Using Only Macro- and Microtexture Measurements," *J. Transport. Eng.*, Vol. 131, No. 4, 2005, pp. 311–319, https://doi.org/10.1061/(ASCE)0733-947X(2005)131:4(311)

[5] El Gendy, A. and Shalaby, A., "Mean Profile Depth of Pavement Surface Macrotexture Using Photometric Stereo Techniques," *J. Transport. Eng.*, Vol. 133, No. 7, 2007, pp. 433–440, https://doi.org/10.1061/(ASCE)0733-947X(2007)133:7(433)

[6] El Gendy, A. and Shalaby, A., "Image Requirements for Three-Dimensional Measurements of Pavement Macrotexture," *Transport. Res. Rec.*, No. 2068, 2008, pp. 126–134, https://doi.org/10.3141/2068-14

[7] Henry, J. J., 2000, "Evaluation of Pavement Friction Characteristics," *NCHRP Synthesis 291*, Transportation Research Board, National Research Council, Washington, DC.

[8] Noyce, D. A., Bahia, H. U., Yambó, J. M., and Kim, G., "Incorporating Road Safety into Pavement Management: Maximizing Asphalt Pavement Surface Friction for Road Safety Improvements," *MRUTC04-04, Report No. 2007-005*, Midwest Regional University Transportation Center, Madison, WI, 2007.

[9] Huang, Y., Copenhaver, T., and Hempel, P., "Texas Department of Transportation 3D Transverse Profiling System for High-Speed Rut Measurement," *J. Infrastruct. Syst.*, Vol. 19, No. 2, 2013, pp. 221–230, https://doi.org/10.1061/(ASCE)IS.1943-555X.0000088

[10] Hanson, D. I. and Prowell, B. D., "Evaluation of Circular Texture Meter for Measuring Surface Texture of Pavements," *NCAT Report 04–05*, National Center for Asphalt Technology, Auburn, AL, 2004.

[11] Abe, H., Henry, J. J., Tamai, A., and Wambold, J., "Measurement of Pavement Macrotexture with Circular Texture Meter," *Transport. Res. Rec.*, No. 1764, 2001, pp. 201–209, https://doi.org/10.3141/1764-21

[12] Bubaker-Isheil, H., Serri, J., and Fontaine, J. F., "3D Displacement Field Measurement with Correlation Based on the Micro-Geometrical Surface Texture," *Optics Lasers Eng.*, Vol. 49, No. 7, 2011, pp. 793–803, https://doi.org/10.1016/j.optlaseng.2011.03.007

[13] Jiang, Z., Shi, W., Han, D., Sun, W., and Liu, L., "Three-Dimensional Microscopy Image System Based on Depth from Focus," *Comput. Tomogr. Theory Appl.*, Vol. 13, No. 4, 2004, pp. 9–15.

[14] Li, S., Kwok, J. T., and Wang, Y., "Multi-Focus Image Fusion using Artificial Neural Networks," *Pattern Recog. Lett.*, Vol. 23, No. 8, 2002, pp. 985–997, https://doi.org/10.1016/S0167-8655(02)00029-6

[15] Malikas, C., "Comparison of Polymers: A New Application of Shape from Focus," *IEEE Trans. Syst., Man, Cybernet, Part C (Appl. Rev.)*, Vol. 39, No. 2, 2009, pp. 246–250, https://doi.org/10.1109/TSMCC.2008.2001714

[16] Scott, W. and Donovan, A., "Comparison of Surface Texture Measurement by Stylus and Fiber Optic Transducers," *J. Test. Eval.*, Vol. 26, No. 1, 1998, pp. 70–78, https://doi.org/10.1520/JTE11972J

[17] Hu, C., Youtcheff, J., Wang, D., Zhang, X., Kutay, E., and Thyagarajan, S., "Characterization of Asphalt Mixture Homogeneity Based on X-Ray Computed Tomography," *J. Test. Eval.*, Vol. 40, No. 7, 2012, pp. 663–681.

[18] Han, D., "Research on Image Fusion Sequences and Three Dimensional Measurement Technology Base on Depth from Focus," Beijing University of Aeronautics and Astronautics, Beijing, 2004.